An integrated Building-to-Grid model for evaluation of energy arbitrage value of thermal storage

Muhammad Bashar Anwar,
Carlos Andrade Cabrera,
Olivier Neu, Mark O'Malley
Energy Institute, University College Dublin,
Dublin, Ireland
muhammad.anwar@ucdconnect.ie
carlos.andradecabrera@ucdconnect.ie
olivier.neu@ucdconnect.ie
mark.omalley@ucd.ie

Daniel J. Burke
Electrical Engineer,
Warwick, UK
dnlbrk157@gmail.com

***Abstract*—Thermal Electric Storage (TES) has emerged as a promising technology for enhancing the flexibility of the built environment to participate in active Demand Side Management (DSM). These devices allow the decoupling of intra-day scheduling of electric power demand from the time of thermal energy end-use. Therefore, if enabled with communication with the grid, these devices can facilitate load shifting and energy arbitrage. This study evaluates the energy arbitrage value of smart TES devices in residential buildings across Ireland. A Building-to-Grid (B2G) model has been developed which integrates the buildings thermal dynamics and end-use constraints with the power systems economic dispatch model. The thermal behavior of the houses and the TES space heater and hot water tank is modeled through linear state space models for three different mid-flat archetypes. The optimization results show the load shifting and arbitrage potential of TES and its impacts on wind curtailment considering various penetration levels of these devices.**

***Index Terms*—Building-to Grid model, Demand Side Management, Electric Heating, Energy Arbitrage, Smart Thermal Storage.**

NOMENCLATURE

Constants

α_n	Number of Houses for Archetype n
Δj	Time Step (h)
η_n	Hourly Energy Retention Parameter of TES Space Heater
$\pi_{g,i}$	Conventional Generator Operating Cost (e/MWh)
ρ	Density of Water (kg/m^3)
c_p	Specific Heat Capacity of Water (MWh/kgK)
D^j_{base}	Non-heating Electricity Base Load (MW)
E^{max}_n	Maximum Storage Capability of TES Space Heater (MWh)
g^{max}_i	Conventional Generator Maximum Power Rating (MW)
g^{min}_i	Conventional Generator Minimum Stable Level(MW)
H^{max}_n	Electric Power Rating of DHW Heater (MW)
I	Number of Conventional Generators
J	Optimization time horizon
N	Number of Archetypes
O^j_n	Binary Indicator for Active Occupancy)
Q^{max}_n	Maximum Heat Output Capability of TES Space Heater(MWh)
$r_{dn,i}$	Conventional Generator Ramp Up Limit (MW)
$r_{up,i}$	Conventional Generator Ramp Up Limit (MW)
S^{max}_n	Electric Power Rating of TES Space Heater(MW)
$snsp_{lim}$	System Non-Synchronous Penetration Limit
$T_{n,in}$	Cold Water Inlet Temperature (°C)
$T^{max}_{n,r}$	Maximum Room Temperature (°C)
$T^{min}_{n,r}$	Minimum Room Temperature (°C)
$T^{max}_{n,t}$	Maximum DHW Tank Temperature (°C)
$T^{min}_{n,t}$	Minimum DHW Tank Temperature (°C)
UA_n	Heat Transfer Coefficient of DHW Tank (MW/m^2K)
$V^j_{dem,n}$	Hot Water Demand of archetype n at time j (m^3)
$V_{n,t}$	DHW Tank Volume (m^3)
W^j_{av}	Available Wind Power (MW)

Variables

E^j_n	Energy Level of TES Space Heater in archetype n at time j (MWh)
g^j_i	Power Output of Generator i at time j (MW)
H^j_n	DHW Power Consumption of archetype n at time j (MW)
P^j_n	Total Heating Power Consumption of archetype n at time j (MW)
Q^j_n	Active Heat Output of TES Space Heater in archetype n at time j (MWh)
$Q^j_{n,heat}$	Total Heat Input in archetype n at time j (MWh)
$Q^j_{n,loss}$	Storage Heat Losses of TES Space Heater in archetype n at time j (MWh)
S^j_n	Space Heating Power Consumption of archetype n at time j (MW)
$T^j_{n,r}$	Room Temperature of archetype n at time j (°C)

This work is part of the RealValue project. This project has received funding from the European Unions Horizon 2020 research and innovation programme under grant agreement No 646116.

$T^j_{n,t}$ DHW Tank Temperature of archetype n at time j (°C)
w^j Total Wind Power Output at time j (MW)

I. Introduction

Demand Side Management (DSM) refers to a wide array of programs designed by the utility companies to alter the time and/or quantity of electricity demand in order to achieve beneficial changes in the system load shape while increasing customers' satisfaction [1]. Effective DSM can yield several benefits including lower electricity generation costs, reduced requirement for investments in generation, transmission and distribution assets, and mitigation of the challenges introduced due to grid integration of highly intermittent non-synchronous renewables [2]. This study focuses on the evaluation of load shifting and energy arbitrage value of DSM, particularly thermal demand, through optimal operation of Thermal Electric Storage (TES).

Space and water heating demand contributes to approximately 80% of the final energy consumption in domestic buildings in Europe [3]. Therefore, environmental and energy security targets set by the European Climate Foundation (ECF) have encouraged the electrification of heat supply in the residential sector [4]. TES for space and water heating has emerged as a promising electricity-to-heat technology with the potential of enabling the participation of thermal demand in active Demand Side Management (DSM). These devices allow the decoupling of intra-day scheduling of electric power demand from the time of thermal energy end-use while satisfying the consumers' thermal comfort requirements. Therefore, if enabled with communication with the grid, these devices can facilitate load shifting and energy arbitrage.

Most of the literature which evaluate the benefits of flexible thermal demand simplify either the demand or the supply side models. For assessment of system-wide effects of flexible loads, most studies implement Unit Commitment/Economic Dispatch (UC/ED) tools with representation of flexible demand using price elasticity or virtual generator models (VGM). Price-elasticity models represent change in demand as a response to change in electricity prices based on the historical/simulated values of elasticities. In [5] , the authors integrate a full model of price responsive shiftable demand in a Security Constrained Unit Commitment (SCUC) model to assess the value of demand bidding in both the energy and reserve market. Similarly, the impact of real time pricing on the utilization of wind power was studied in [6] using price elastic demand. Virtual Generator Models represent demand as electricity generation/storage units with negative power outputs and operational constraints based on the type of demand and customer preferences. Authors of [7] use VGM to model flexible demand for the co-optimization of energy and reserve markets with participation from both the supply and the demand sides. Similarly, representation of large, spatially-distributed populations of heat pumps, electric vehicles, and electrolyzers in Security Constrained Economic Dispatch (SCED) using VGM has been presented in [8]. However, such simplified representation of demand fails to take into account the impact of demand response on the consumers and does not guarantee fulfillment of consumers' thermal comfort constraints.

On the other hand, studies which focus on the impact of demand side measures on consumers tend to have detailed physical/thermal demand models with simplified representation of the supply side, usually using price signals. In [9], the authors optimize the control of partial storage electric space heating to minimize the total energy cost of customers based on fixed electricity price profiles. The economic value of Heat Pumps (HP) and Electric Boilers (EB) is assessed based on a two-stage stochastic programming model in [10]. The model is employed to optimize the operation of HP and EB along with a Combined Heat and Power (CHP) unit using price signals in the context of a heat market in Denmark. However, using fixed electricity price signals to assess the value of demand response have the drawback of not incorporating the feedback impact of the change in demand on the electricity price. Therefore, such models cannot provide technically valid estimates of the energy arbitrage value of a large fleet of thermal storage.

Recently, some studies have presented joint optimization models which include detailed representation of both the demand and the supply sides. A comparison of heat storage technologies including heat accumulation tanks and passive heat storage coupled with heat pumps in terms of fuel cost savings and wind integration in the Danish system has been presented in [11]. Additionally, [12] explores the merits of using detailed integrated thermal demand and grid side models as compared to either simplified demand and/or supply side models. The authors develop an integrated model of a typical electric power system and thermal demand from buildings using heat pumps and auxiliary electric resistance heaters coupled with hot water tank as storage medium. The comparison highlights the drawbacks of the simplified models as compared to the integrated model in terms of representing the impacts of load shifting on the consumers and also on the supply mix and electricity prices.

The Building-to-Grid (B2G) model developed in this study takes a similar modeling approach by integrating the buildings' thermal dynamics and end-use constraints with the power systems economic dispatch model. However, in comparison to [12], the novel contributions of this study are as follows: three different archetypes have been used; an annual system-wide analysis for the All Island Power System (AIPS) has been conducted to have a detailed evaluation of the annual energy arbitrage value of TES; instead of heat pumps, Smart Electric Thermal Storage (SETS) devices [13] have been used as the electricity-to-heat technology. SETS space heaters contain a highly insulated solid thermal energy storage core which enables the conversion of electrical energy into thermal energy stored in an efficient manner for use at a later time. SETS water cylinders use the same basic principle, except that the energy is stored in water rather than a solid medium. Both the storage systems share the same communications and control architecture [13] and therefore have energy arbitrage potential. An initial assessment of the value of SETS devices in AIPS

has been presented in [14], in which the heating demand is modeled as a fixed time series. This paper builds upon this assessment by implementing state-space models for space and water heating demands for the different archetypes in order to better represent the thermal dynamics, thermal comfort constraints and passive storage potential in the building fabric.

The rest of the paper is organized as follows. Section II presents the modeling details and methodology for the development of the B2G model. Section III discusses the results and the performance of TES subject to various sensitivities. And finally, Section IV concludes the findings of this study.

II. Methodology

This section presents the modeling details of building thermal characteristics, domestic hot water demand and subsequently the integrated B2G optimization model.

A. Building State Space Model

Three EnergyPlus mid-flat archetypes [15], were used to generate synthetic building performance data. The first two are representative of double glazed ($U_{win} = 2.88\,[W/m^2K]$, $g_{win} = 0.759$) uninsulated apartments built before 1985. The first model features external hollow brick walls ($U_{wall} = 2.6\,[W/m^2K]$), whereas the second model features cavity walls ($U_{wall} = 2.5\,[W/m^2K]$). Both archetypes are modelled with a moderate infiltration rate (0.35 ACH per zone). The third archetype is representative of recent constructions (1995 onwards) which feature energy efficiency measures such as insulated external walls ($U_{wall} = 0.19\,[W/m^2K]$), triple glazing windows ($U_{win} = 2.88\,[W/m^2K]$, $g_{win} = 0.759$) and low infiltration rates (0.19 ACH per zone). The surfaces adjacent to other apartments are considered as adiabatic, with the exception of the East-facing surfaces, which have a boundary condition of $18°C$ (conditioned hallway). Weather conditions correspond to the Dublin IWEC weather file [16]. The archetypes are modeled using the thermal network topology shown in Figure 1. Node T_{amb} represents the dry-bulb outdoor temperature. Nodes C_{w1} and C_{w2} and resistances R_{ext_1}, R_{ext_2} and R_{ext_3} model the two leaves of the external walls. The wall solar gains, $Q_{s,wall}$, are applied directly to node C_{w1}. C_r represents the capacitance of the air mass with room temperature T_r. Node C_{int} and resistance R_{int} model the thermal mass of the internal partitions and other slow dynamics. The window solar gains $Q_{s,win}$ and the heating power input Q_{heat} are split between C_r and C_{int} via parameters f_1 and f_2. The proposed model topology is shown in Figure 1. Node C_{hall} and resistances R_{hall_1} and R_{hall_2} model the internal walls adjacent to the hallway.

After expanding the heat balance equations for all the nodes, re-ordering terms, and discretizing the resulting continuous-time model, the building energy model can be represented by the state-space equation:

$$x_n^{j+1} = A_n\, x_n^j + B_{n,u}\, Q_{n,heat}^j + B_{n,d}\,[T_{amb,k}\; Solar_{West,k}\; Solar_{North,k}\; T_{hall}] \quad (1)$$

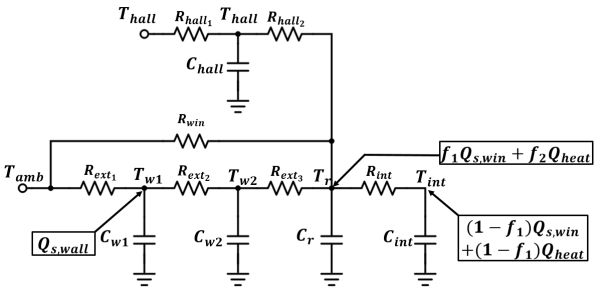

Fig. 1: Proposed heterogeneous lumped parameters building model topology

where $x_n^j = \begin{bmatrix} T_{n,w_1}^j & T_{n,w2i}^j & T_{n,r}^j & T_{n,int}^j & T_{n,hall}^j \end{bmatrix}$ is the state vector, A_n, $B_{n,u}$ and $B_{n,d}$ as state, input and disturbance matrices and $Solar_{West}$ and $Solar_{North}$ are the global solar radiation incident in the the West and North facades, respectively. This model was calibrated using Particle Swarm Optimization (PSO) using the MATLAB Global Optimization toolbox ([17]).

B. Domestic Hot Water Demand Model

The analytical domestic hot water (DHW) demand profiles for the midflat archetypes are developed using an occupant focused approach based on Time-of-Use Survey (TUS) data. The reference dwellings are considered over different construction periods, representative of the majority of the Irish midflats. Building Performance Simulations of these archetypes are then modeled by integrating high space and time resolution operational data. Activity specific DHW consumption profiles are obtained using the bottom-up approach developed by Neu et al. [18], which is based on the application of Markov Chain Monte Carlo techniques to TUS data [19]. This approach combines the average daily DHW consumptions, as estimated through the UK SAP procedure [20], with the probability distributions for the corresponding TUS hot water draw activities. The profiles capture variations in DHW consumption, heat demand and energy usage for DHW heating, with a 15-minute time-resolution. Results for the annual heating demands are verified by comparing them with those estimated through the DEAP approach.

C. Building-to-Grid Model

The Building-to-Grid (B2G) model is fundamentally an economic dispatch model, which minimizes total cost of electricity generation, subject to power system operational constraints, technical constraints of the generating units and thermal demand constraints of the considered building archetypes. Integration of the building thermal dynamics with the power system economic dispatch models facilitates the co-optimization of generation scheduling with power consumption scheduling of the TES devices. The B2G model is formulated as follows:

$$min \sum_{j=1}^{J} \sum_{i=1}^{I} (\pi_{g,i}.g_i^j) \quad (2)$$

subject to:

$$\sum_{i=1}^{I} g_i^j + w^j = \sum_{n=1}^{N} (\alpha_n . P_n^j) + D_{base}^j, \quad \forall j \in [1, J] \tag{3}$$

$$w^j \leq snsp_{lim} . \left(\sum_{n=1}^{N} (\alpha_n . P_n^j) + D_{base}^j \right), \quad \forall j \in [1, J] \tag{4}$$

$$g_i^{min} \leq g_i^j \leq g_i^{max}, \quad \forall j \in [1, J] \quad \forall i \in [1, I] \tag{5}$$

$$g_i^j - g_i^{j-1} \leq r_{up,i}, \quad \forall j \in [1, J] \quad \forall i \in [1, I] \tag{6}$$

$$g_i^{j-1} - g_i^j \leq r_{dn,i}, \quad \forall j \in [1, J] \quad \forall i \in [1, I] \tag{7}$$

$$w^j \leq W_{av}^j, \quad \forall j \in [1, J] \tag{8}$$

$$P_n^j = S_n^j + H_n^j, \quad \forall j \in [1, J] \quad \forall n \in [1, N] \tag{9}$$

$$T_{n,r}^{min} . O_n^j \leq T_{n,r}^j . O_n^j \leq T_{n,r}^{max} . O_n^j, \quad \forall j \in [1, J] \quad \forall n \in [1, N] \tag{10}$$

$$E_n^{j+1} = E_n^j + S_n^j . \Delta j - Q_n^j - Q_{n,loss}^j, \quad \forall j \in [1, J] \quad \forall n \in [1, N] \tag{11}$$

$$Q_{n,loss}^j = (1 - \eta_n) . E_n^j, \quad \forall j \in [1, J] \quad \forall n \in [1, N] \tag{12}$$

$$Q_{n,heat}^j = Q_n^j + Q_{n,loss}^j, \quad \forall j \in [1, J] \quad \forall n \in [1, N] \tag{13}$$

$$0 \leq Q_n^j \leq Q_n^{max}, \quad \forall j \in [1, J] \quad \forall n \in [1, N] \tag{14}$$

$$0 \leq S_n^j \leq S_n^{max}, \quad \forall j \in [1, J] \quad \forall n \in [1, N] \tag{15}$$

$$0 \leq E_n^j \leq E_n^{max}, \quad \forall j \in [1, J] \quad \forall n \in [1, N] \tag{16}$$

$$\rho c_p V_{n,t} \frac{T_{n,t}^{j+1} - T_{n,t}^j}{\Delta j} = H_n^j - UA_n . (T_{n,t}^j - T_{n,r}^j) - \rho c_p V_{dem,n}^j . (T_{n,t}^j - T_{n,in}), \quad \forall j \in [1, J] \quad \forall n \in [1, N] \tag{17}$$

$$T_{n,t}^{min} \leq T_{n,t}^j \leq T_{n,t}^{max}, \quad \forall j \in [1, J] \quad \forall n \in [1, N] \tag{18}$$

$$0 \leq H_n^j \leq H_n^{max}, \quad \forall j \in [1, J] \quad \forall n \in [1, N] \tag{19}$$

The objective function (2) of the B2G model minimizes the daily electricity generation cost, which is the summation of conventional generation costs. The cost of conventional generation takes into account the fuel and carbon emissions costs. Eqs. (3) and (4) represent the power system operational constraints. (3) is the power balance constraint which ensures that the total electricity generation equals the total demand at all times. The total electricity demand is represented as the sum of the fixed baseline demand (excluding the heating load for the considered archetypes) and the flexible heating demand. (4) constrains the wind generation to be within the System Non-Synchronous Penetration (SNSP) limit, which is defined as the ratio of non-synchronous generation (wind and HVDC imports) to demand plus HVDC exports [21]. Eqs. (5) - (7) model the technical constraints of all the conventional generators. (5) ensures that the electricity generation of each generator is within its minimum and maximum power production limits. Considering that the B2G is a linear model, the minimum operation limits for all generators have been relaxed and set to $0MW$ in order to avoid the need to keep all the generators on at all times. (6) and (7) represent the ramp-up and ramp-down constraints for the generators, respectively. (8) limits the wind power production to be within the available wind power for the given time interval.

Eqs. (9)-(19) express the space and water heating constraints for the considered archetypes. (9) describes the total heating load for each dwelling to be the summation of the space heating and DHW electricity consumption. (10) constrains the room temperature, $T_{b,r}^j$, to be within the thermal comfort limits during active occupancy periods. $T_{b,r}^j$ is determined using the state space model described in Section II-A. (11) models the evolution of the storage level of the TES for space heating. TES space heating storage losses are calculated using (12). (13) describes the total space heating input to be the summation of active heat output of the TES and the storage heat losses. Eqs. (14)-(16) constrain the active heat output, electric power input and storage level of the TES space heaters to be within their respective rated values. (17) represents the temperature evolution of the DHW storage tank as a state space model. A simple one node perfectly stirred water tank model is considered. The first term on the right side of the equation represents the DHW input power, the second term represents the heat losses from the tank to the surroundings while the third term models the heat loss in the event of hot water draw, during which the cold water at the inlet, $T_{b,in}$, replaces an equivalent amount of water. (18) constrains the DHW tank temperature to be within the prescribed operation limits and (19) limits the DHW input power to be within the rated values.

The B2G model has an hourly time-resolution and is solved with a look-ahead horizon of 48 hours assuming perfect forecast. The results for the first 24 of those 48 hours are stored, before rolling on to the next day of the year. This rolling-optimization approach allows the B2G model to consider keeping some storage in the TES at the end of the day depending on the conditions the next day. The model is implemented in GAMS 24.6 and MATLAB 2013a, using the MATLAB-GAMS coupling as described in [22].

III. Results and Discussion

Th developed B2G model has been used to conduct an annual evaluation of the energy arbitrage potential of TES in AIPS. The conventional generation portfolio of the AIPS including the number of units, heat rates and other important characteristicshave been modeled according to [23]. The associated fuel costs of the various fuels for the year 2012 are obtained from [24] and the fuel carbon intensities are based on [25]. Tables I and II present the characteristics of the TES space and water devices for each of the considered archetypes based on the maximum daily heating requirements and SETS device specifications [15]. Key modeling assumptions made in this study are presented in Table III.

Figs. 2 and 3 depict the performance of the TES devices for a typical day in the heating season with 50% of the midflats heated with TES devices. The remaining proportion of midflats have Direct Resistive Heaters (DRH) for space

TABLE I: TES Space Heating Specifications for Midflats

	New	Old cavity	Old hollow
Number of homes (in 1000's)	34.883	14.403	25.731
Number of SETS units per home	2	2	2
Elec power rating per SETS unit (kW)	1.56	2.2	2.2
Energy storage capability per SETS unit (kWh)	10.9	15.4	15.4
Heat output capability per SETS unit (kW)	0.7	1.2	1.2
Hourly efficiency parameter	0.972	0.975	0.975

TABLE II: TES DHW Specifications for Midflats

	New	Old cavity	Old hollow
Number of SETS units per home	1	1	1
Elec power rating per SETS unit (kW)	3	3	3
Mass of water in tank (kg)	250	250	250
UA value (W/K)	1.4315	1.4315	1.4315
Min. tank temp (°C)	50	50	50
Max. tank temp (°C)	70	70	70

and water heating. Fig. 2 shows the indoor and DHW tank temperature evolution and their corresponding power consumption for a day. It can be observed that the TES is able to maintain the room temperatures within the thermal comfort range from 20 - 25 $°C$ during periods of active occupancy (i.e. 07:00-09:00 and 17:00-23:00) for all three of the midflat archetypes. Similarly the hot water temperature remains within the prescribed range from 50 - 70 $°C$ throughout the day. The power consumption profiles indicate that the TES charge during 01:00 - 04:00 at night before the actual time of thermal end-use, thereby shifting the load and providing energy arbitrage. It is also interesting to note that the rolling optimization approach of the B2G model allows retention of some storage in the TES at the end to be used the next day.

Fig. 3 shows the AIPS electricity demand and wind power utilization for the given day. It can be observed that with the implementation of TES devices, the total demand can be reduced during the evening peak. Additionally, Fig. 3b shows that due to the 50% SNSP limit, there is significant wind curtailment during the early morning period. However, as the TES devices charge during this period (see Fig.2), the total demand increases as compared to the demand when all the midflats are heated with DRH. This results in a decrease in wind curtailment levels and hence, depicts the potential of TES in facilitating greater utilization of renewable energy.

TABLE III: Key Modeling Assumptions

AIPS Peak Load (MW)	7300
AIPS Wind Capacity (MW)	4000
SNSP Limit	0.5
Carbon Price (€/tonne)	20
Min. Indoor Temperature (°C)	20
Max. Indoor Temperature (°C)	25
Active Occupancy Periods	07:00-09:00 and 17:00-23:00

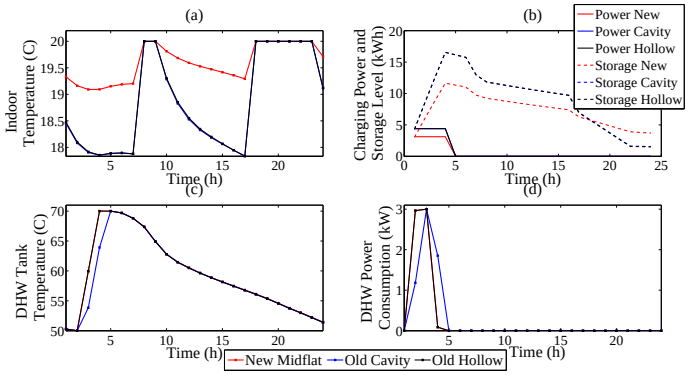

Fig. 2: TES Temperature and Power Consumption Profiles

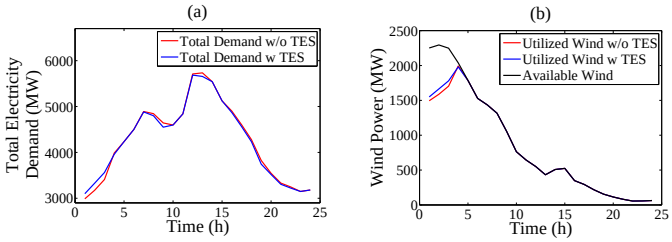

Fig. 3: Total Electricity Demand and Wind Profiles

Fig. 4 shows the annual performance of TES in terms of reducing generation costs, wind curtailment levels and system peak load under different levels of TES penetration and SNSP limits. Considering different penetration levels of TES devices can help in understanding the potential of these devices in comparison to DRH and varying the SNSP limits facilitates the analysis of future potential of TES with greater levels of renewable energy. It can be observed from Fig. 4a that as the proportion of midflats heated with TES increases, there is a steady reduction in the annual electricity generation costs for all levels of SNSP limits. The maximum annual cost savings potential (i.e. with 100% TES devices) is circa € 9.3 million per annum as compared to the case where all midflats are installed with DRH. The magnitude of the cost savings remains approximately the same across all SNSP limits which shows that TES devices have robust arbitrage potential even under low cost high renewables future power systems. Fig. 4b shows that although increasing penetration of TES devices reduces wind curtailment levels for all SNSP limits, however, the magnitude of this reduction falls as SNSP limits increase. This can be attributed to the fact that curtailment levels are already under 2% at 75% SNSP limit and DRH can also benefit from increase in wind energy. Additionally, it is important to note that only midflats have been considered in this study which account for only about 70,000 houses in Ireland. As a result there is not enough flexible demand to further reduce curtailment levels at high SNSP limits. Fig. 4c highlights the peak shaving potential of TES devices. It can be observed that

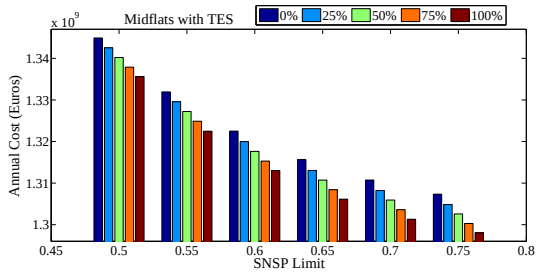

(a) AIPS Annual Electricity Generation Cost

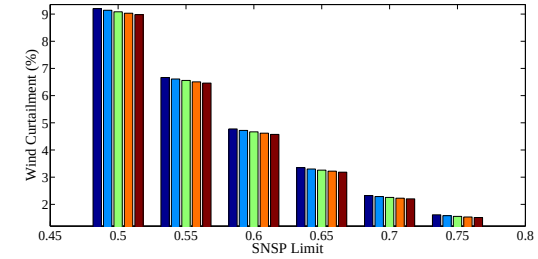

(b) Total Annual Wind Curtailment

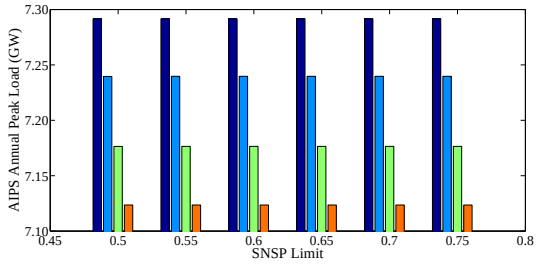

(c) AIPS Annual Peak Load

Fig. 4: Annual Performance of TES devices under various sensitivities

annual peak load can be noticeably reduced with TES devices. Indeed, approximately 180 MW of peak load can be reduced even only midflats are heated with TES devices. However, increasing SNSP limits does not have any effect on peak load reduction potential of TES. Hence, TES can play an important role in reducing not only operational costs but also investment costs in generation and transmission infrastructure.

IV. Conclusion

This paper presents an evaluation of energy arbitrage and load shifting capability of smart TES devices in residential dwellings. A B2G model is developed which co-optimizes the power systems economic dispatch with the characteristics and requirements of the residential electric space and water heating demand. The B2G model is implemented for the AIPS considering three midflat archetypes. The results highlight the energy arbitrage potential of TES in terms of significant generation cost savings, greater utilization of wind generation and reduction in peak load under different scenarios.

Future work will incorporate other residential archetypes and different occupancy patterns in the B2G model to account for the rest of the domestic heating demand. Additionally, potential of TES devices for providing ancillary services, such as operating reserves, will also be studied.

References

[1] C. W. Gellings and J. Chamberlin, "Demand-side management," 1988.

[2] G. Strbac, "Demand side management: Benefits and challenges," *Energy policy*, vol. 36, no. 12, pp. 4419–4426, 2008.

[3] IEA, "Energy balances of oecd countries 2014," 2014.

[4] E. C. F. (ECF), "Eu roadmap 2050, a practical guide to a prosperous, low-carbon europe e technical analysis," 2010.

[5] G. Liu and K. Tomsovic, "A full demand response model in co-optimized energy and reserve market," *Electric Power Systems Research*, vol. 111, pp. 62–70, 2014.

[6] R. Sioshansi and W. Short, "Evaluating the impacts of real-time pricing on the usage of wind generation," *IEEE Transactions on Power Systems*, vol. 24, no. 2, pp. 516–524, 2009.

[7] Y. T. Tan and D. S. Kirschen, "Co-optimization of energy and reserve in electricity markets with demand-side participation in reserve services," in *2006 IEEE PES power systems conference and exposition*. IEEE, 2006, pp. 1182–1189.

[8] D. Wang, S. Parkinson, W. Miao, H. Jia, C. Crawford, and N. Djilali, "Hierarchical market integration of responsive loads as spinning reserve," *Applied energy*, vol. 104, pp. 229–238, 2013.

[9] M. Ali, J. Jokisalo, K. Siren, and M. Lehtonen, "Combining the demand response of direct electric space heating and partial thermal storage using lp optimization," *Electric Power Systems Research*, vol. 106, pp. 160–167, 2014.

[10] M. G. Nielsen, J. M. Morales, M. Zugno, T. E. Pedersen, and H. Madsen, "Economic valuation of heat pumps and electric boilers in the danish energy system," *Applied Energy*, vol. 167, pp. 189–200, 2016.

[11] K. Hedegaard, B. V. Mathiesen, H. Lund, and P. Heiselberg, "Wind power integration using individual heat pumps–analysis of different heat storage options," *Energy*, vol. 47, no. 1, pp. 284–293, 2012.

[12] D. Patteeuw, K. Bruninx, A. Arteconi, E. Delarue, W. Dhaeseleer, and L. Helsen, "Integrated modeling of active demand response with electric heating systems coupled to thermal energy storage systems," *Applied Energy*, vol. 151, pp. 306–319, 2015.

[13] B. i. t. G. Jillis Raadschelders, Friso Sikkema, "Potential for smart electric thermal storage contributing to a low carbon energy system," 2013.

[14] D. Burke, O. Neu, S. Nolan, and H. Qazi, "Initial cost benefit analysis comparison for domestic smart electric thermal storage (sets) vs direct resistive heating (drh) on the irish all-island power system," *Electricity Research Centre, UCD*, Feb 2014.

[15] O. Neu, B. Sherlock, S. Oxizidis, D. Flynn, and D. Finn, "Developing building archetypes for electrical load shifting assessment: Analysis of irish residential stock," *CIBSE ASHRAE Technical Symposium*, April 2014.

[16] ASHRAE, "International Weather for Energy Calculations (IWEC Weather Files) Users Manual and CD-ROM," ASHRAE, Atlanta, Tech. Rep., 2001.

[17] Mathworks, "Global Optimization Toolbox - User's Guide," Tech. Rep., 2015.

[18] O. Neu, S. Oxizidis, D. Flynn, and D. Finn, "Utilising time of use surveys to predict domestic hot water consumption and heat demand profiles of residential building stocks," *British Journal of Environment & Climate Change*, vol. 6(2), pp. 77–89, 2016.

[19] I. Richardson, M. Thomson, and D. Infield, "A high-resolution domestic building occupancy model for energy demand simulations," *Energy and buildings*, vol. 40, no. 8, pp. 1560–1566, 2008.

[20] *The Government's standard assessment procedure for energy rating of dwellings - SAP 2009 version 9.90.* Building Research Establishment, 2011.

[21] EIRGRID and SONI, "Annual Renewable Energy Constraint and Curtailment Report," 2014.

[22] M. C. Ferris, R. Jain, and S. Dirkse. (2011) GDXMRW: Interfacing gams and matlab. [Online]. Available: http://www.gams.com/dd/docs/tools/gdxmrw.pdf

[23] CER, "2012a. PLEXOS Validation, commission for energy regulation, utility regulator electricity gas water." 2012.

[24] DECC, "Uk department of energy & climate change fossil fuel price projections," 2013.

[25] SEAI, "Carbon emission factors," 2014.